PROGRESS TOWARDS PICOMETER ACCURACY LASER METROLOGY FOR THE SPACE INTERFEROMETRY MISSION – UPDATE FOR ICSO 2004

Peter G. Halverson[1], Oscar Alvarez-Salazar[2], Alireza Azizi[3], Frank Dekens[4], Bijan Nemati[5], Feng Zhao[6]

[1]Jet Propulsion Laboratory (JPL), California Institute of Technology,
4800 Oak Grove Drive, Pasadena, CA 91109 U.S.A, Peter.G.Halverson@jpl.nasa.gov
[2] JPL, Oscar.S.Alvarez-Salazar@jpl.nasa.gov
[3] JPL, Alireza.Azizi@jpl.nasa.gov
[4] JPL, Frank.G.Dekens@jpl.nasa.gov
[5] JPL, Bijan.Nemati@jpl.nasa.gov
[6] JPL, Feng.Zhao@jpl.nasa.gov

ABSTRACT

The Space Interferometry Mission, scheduled for launch in 2008, is an optical stellar interferometer with a 10 meter baseline capable of micro-arcsecond accuracy astrometry. A mission-enabling technology development program conducted at JPL, has yielded the heterodyne interferometric displacement metrology gauges required for monitoring the geometry of optical components of the stellar interferometer, and for maintaining stable starlight fringes. The gauges have <20 picometer linearity, <10 micron absolute accuracy, are stable to <200 pm over the typical SIM observation periods (~1 hour), have the ability to track the motion of mirrors over several meters. We discuss the technology that led to this level of performance: low-cross-talk, low thermal coefficient optics and electronics, active optical alignment, a dual wavelength laser source, and a continuously averaging, high data rate phase measurement technique. These technologies have wide applicability and are already being used outside of the SIM project, such as by the James Webb Space telescope (JWST) and Terrestrial Planet Finder (TPF) missions.

1. INTRODUCTION

The Space Interferometry Mission (SIM) [1,2] will measure the angular positions of ~2000 astronomical objects (mainly stars) for the detection and characterization of planets, gravitational lensing events, black holes and other exotic phenomena. SIM will detect these by their influence on the angular position of the object observed. For example, an earth-sized planet orbiting a nearby star at 1 AU could be detected by the angular "wobble" of the star, about 1 μas (=4.8 picoradians).

SIM measures the relative angles of three stars at a time. Two "guide" stars are needed as a reference to determine the orientation of SIM itself, while the third, "science" star is measured. Each star's angular position is measured by measuring the starlight phase delay between a pair of telescopes joined in an interferometer. Hence to function, SIM needs three starlight interferometers. (A fourth is available for redundancy.)

Metrology is needed to

1. provide knowledge of the angles between each interferometer (called external metrology) and
2. to provide internal calibration of the optical delay in the starlight interferometers (internal metrology).

Fig. 1 is a cut-away view showing the four stellar interferometers (two guide, and two science) and the external metrology beams that link them together in a three-dimensional virtual "truss" of positional information.

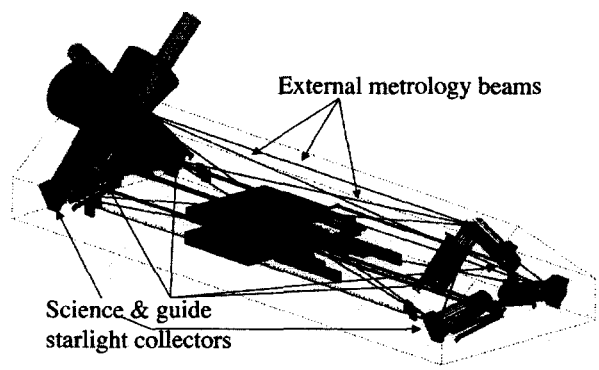

Fig. 1. SIM instrument layout. Blue indicates path of science starlight, green of guide starlight. Red indicates external metrology laser beams which measure distances between fiducials. The long dimension of the spacecraft is ~10 meters. Cones indicate the science and guide field-of-regard for the left side collectors. The right side field-of-regard cones, omitted for clarity, view the same portion of the sky.

The performance of SIM is directly related to the accuracy of the metrology. The error in measuring a star's location is roughly $\varepsilon(L)/D$ where $\varepsilon(L)$ is the typical metrology error and D=10 meters is the baseline, the distance between the starlight interferometer telescopes. For an astrometric accuracy of 5 picoradians, we would need to limit errors to 50

pm. Because of other sources, the contribution from metrology should actually be less that this.

Table 1. SIM metrology requirements. Number in parentheses indicate *old* requirements, as of 2000.

	Internal metrology requirement	External metrology requirement
Number of gauges	4 (8)	19 (42)
Number of gauges for mission success*	3 (6)	12 (24)
Distance between fiducials	20 m	Shortest: 2.5 m (4 m) Longest: 10.6 m (12 m)
Motion; ranges of distances	~2.6 m	~10 microns
Velocity	2 cm/s while changing stars, 1 micron/sec while observing	
Accuracy (absolute)	Not needed.	3 microns rms
Accuracy relative	~57 (15) pm rms, 1 hour time scale; ~10 (8) pm rms, 90 s time scale, *after removal of linear component***	
Temp. coefficient	2 pm/mK (soak); 50 pm/mK (sensitivity to gradients)	

* Assumes dispersed failures. Some failures are more tolerable than others.

** Modified observing schedule will allow off-line the removal of drifts that are linear in time.

Hence the metrology needs of SIM, listed in Table 1, are demanding and must be addressed for the mission to succeed. Early progress was described in the previous ICSO conference [3] and more of the real issues will be seen in another talk at this conference [4]. SIM metrology is still evolving in the laboratory and its final configuration is not yet known, but the lessons learned in ongoing experiments should apply.

It should also be noted that the accuracy requirements for a single gauge are relative to the other gauges, in the sense that if *all* gauges under/overestimate distances proportionally, the derived knowledge of the *angular shape* of SIM would be unaffected. Given that SIM's astrometric goals only require knowledge of the angles between the optical systems, to first order the need for laser source long-term wavelength stability is relaxed.

Although the distances the external metrology measures are several meters, the required dynamic range is small, a few microns, depending on the stiffness of the spacecraft .

Internal metrology has similar accuracy requirements as external metrology but with a dynamic range of a few meters due to optical delay line motion. It must coexist with the starlight constraining its aperture. A separate experiment, the Diffraction Testbed, will investigate internal metrology issues and test and various proposed solutions.

1.1 General description of SIM metrology

Displacement metrology for the SIM testbeds (see Fig. 2) consists of a laser source [5] which supplies two λ=1.3 micron outputs with a small frequency difference F_{HET} which can be anywhere from 2 to 1000 kHz, the range of the phasemeter. The two frequency outputs serve as local oscillator (LO) and Probe sources. These outputs are carried to a metrology interferometer head (not to be confused with the *starlight* interferometers) by polarization maintaining (PM) fibers. If the experiment is inside a vacuum chamber, the fibers travel though a vacuum port to reach the metrology interferometers. The final three meters use *polarizing* fiber to remove energy from the "wrong" (fast) polarization axis before reaching the interferometers. The reason for this will be discussed later.

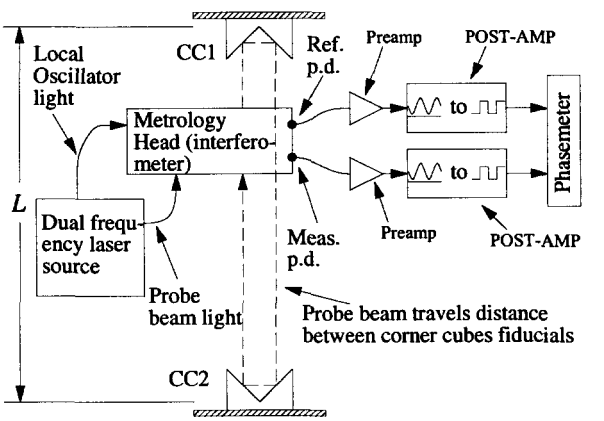

Fig. 2. Metrology gauge for measuring a single distance *L*. SIM uses 19 such gauges for external metrology and 4 for internal, starlight path, metrology.

Fig. 2 shows only one metrology gauge, but SIM will have 19 external gauges, which must work together to create a consistent three-dimensional shape, accurate to a few tens of picometers. The first step in showing that such a truss could be built was demonstrating close agreement between *pairs* of gauges. This was done in the Two-Gauge testbed [6], whose results are that the current gauges have

1. non-linearity < 22 pm for 10 micron displacements,
2. thermal sensitivity ~8 pm/mK,
3. drift ~300 pm/hour.

It should be noted that the cause of the drift is understood and will be corrected and that because of changes in the way the metrology data will be used, it would not be fatal to SIM even if it persisted. Similarly, we believe the thermal sensitivity can be easily reduced in the next generation of gauges.

1.2 Developments in SIM metrology

SIM metrology has evolved since the previous ICSO conference in the following significant ways:

1. Improvement in the astrometric observing plan now allow first-order removal of metrology drift. Similarly, errors that are linearly dependant on observing direction can be removed in data analysis [7].
2. To reduce cyclic non-linearity, the use of polarization as a means to control probe and reference beams has been replaced with physical beam separations.
3. Active alignment of metrology beams has been successfully implemented.
4. Numerous improvements in the electronics and data processing.
5. The metrology has been to scaled to various large testbeds, and has successfully been implemented as part of a SIM-like truss.

This progress will be discussed below.

2. IMPROVED OBSERVATION SCHEDULE AND ANALYSIS

The order in which astrometric observations are performed has a strong impact on the required stability of the instrument. If the metrology drifts linearly with time, then by "chopping" the observations, alternately observing reference stars and science stars, the metrology error can be removed off-line.

An analogy would be having a meter stick that is growing, but also having a stable reference. We could accurately measure an unknown object with the meter stick by (1) measuring the reference then (2) measuring the unknown and (3) re-measuring the reference. If the time between measurements is constant (or at least known), then we can accurately calculate the unknown length.

In SIM's "narrow-angle" mode [7], which will have 5 picoradian accuracy, the positions of a science star, S, and a group of 5 nearby (within 1 degree) reference stars, R_1, R_2 .. R_5, will be measured in the sequence S-R_1-S-R_2-S-R_3-S-R_4-S-R_5-S. The time between each observation will be ~90 seconds. From the data thus acquired, linear drifts (and also linear field dependencies) will be removable. Hence, the modified SIM error budget allows for linear metrology drift. Of course, an "accelerating" drift would be problematic, and must its effect must be less than 10 pm in 90 seconds.

SIM's "wide angle mode," accurate to 18 picoradians, is similar but with longer times scales to accommodate more targets. Within a 15 degree field of view, 6 grid (reference) stars G_1, G_2 .. G_6 will be measured, followed by N science stars S_1, S_2 .. S_N, followed by a repeated observation of the grid stars. The time scale for this sequence is ~1 hour, during which the non-linear, "accelerating," part of metrology drift must be less than 57 pm.

These observing sequences have been incorporated into the KITE testbed which will be discussed in section 5.

3. MINIMIZING CYCLIC ERROR

An early obstacle to <100 pm accuracy was cyclic error, a repeating non-linearity periodic in $\lambda/2$ fiducial displacement caused by (1) leakage (crosstalk) between the L.O. and Probe beams, (2) electrical crosstalk between the Meas. and Ref. heterodyne signals and (3) computational errors arising from data age when tracking a changing distance. The RMS magnitude of the error from the first two effects may be roughly predicted [8] by the formula

$$\varepsilon = 2^{-1/2}(\lambda/2)(1/2\pi)(v/V) \approx (\lambda/18)(v/V) \qquad (1)$$

Applying this formula with λ=1.3 μm, we find that any leakage or crosstalk above -80 dB will cause ~10 pm cyclic error. From a practical standpoint for SIM, we strive to keep the mixing from any single source below -90 dB so that all sources taken together will be less than -80 dB.

The Two-Gauge testbed was used to confirm the cyclic performance of the gauges: after all the improvements described here, the gauges had cyclic errors that ranged from ~40 pm to <10 pm (the detection threshold). The later production metrology heads had better cyclic error performance.

How this was achieved is discussed below:

3.1 Cyclic Error Due to Beam Leakage

The redesigned metrology [9,10] interferometer shown in Figures 3 and 4 represents a departure from the early SIM design (see for example [11]) in that the separation of the L.O. and Probe beams is no longer accomplished using polarizing beams splitters. Indeed, in the new design, L.O.-Probe. crosstalk is hardly an issue. However in this design, the probe beam is subdivided into an outer portion that travels between the fiducials and an inner portion that remains inside the head. These will form the Meas. and Ref. signals and any leakage (diffraction and scattering could be

causes) between inner and outer beams is a potential new cause of cyclic error. Masks have been added to reduce this leakage to acceptable levels. (The improved cyclic error of the later metrology heads was due to better diffraction blocking masks.)

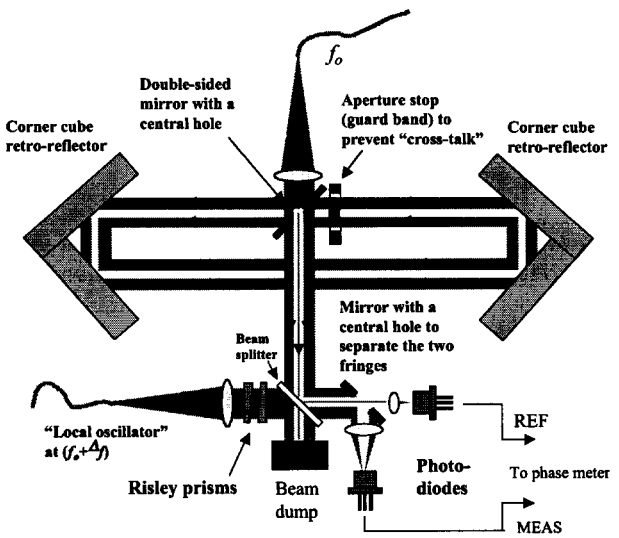

Fig. 3. Block diagram of metrology interferometer. Leakage between the outer beam, which measures distance between corner cube fiducials, and the inner beam, which acts as a reference, results in cyclic error. Similarly, crosstalk between photodiode signals causes cyclic error.

3.2 Cyclic Error Due to Multiple Gauges

As the testing of SIM metrology becomes more realistic on testbeds such as KITE new issues inevitably arise. A new source of cyclic error has been observed that is caused by multiple gauges interrogating a common corner cube fiducial as in Fig. 6 and 7 where, for example, gauges 1,2 and 3 all interrogate the articulated retroreflector cube. If a speck of dust scatters gauge 1's Probe beam into gauge 2, then gauge 2 will experience a cyclic error of magnitude predicted by equation 1. Better than 80 dB gauge-to-gauge isolation is required for <10 pm performance. The solution to this problem will probably involve better control of scattered light and having gauges use non-overlapping portions of the retroreflectors.

3.3 Cyclic error due to electronic crosstalk

Equation 1 also applies to signal mixing downstream of the Ref. and Meas. photodiodes. A continuing effort to upgrade the signal cabling and electronics, which will be presented elsewhere at this conference [12] is resolving this problem.

3.4 Cyclic error due to data age

This problem was noticed while testing the improved, low cyclic error, metrology gauges. It arises when fiducials are moving, and the effective time of measurement is correlated with the instantaneous phase. This effect can be removed in software as described in [8]. It should be noted that this error and the method for its removal are specific to the phase measuring device used at JPL. For current quasi-static experiments such as KITE, the data age issue is not important but it will have to be accounted for in future testbeds, and in SIM itself, where there will be optical delay line motions to compensate for spacecraft orientation drift.

4. MINIMIZING DRIFT

Table 1 includes metrology drift requirements which, to be met, have required the use of low thermal coefficient optics and structures, and special consideration of fiber optics issues, phase measuring electronics and optical alignment.

4.1 Optical configuration for low drift

The metrology head, Figs. 3 and 4, used in SIM testbeds has evolved to the form described in [9,10] which now features

1. no polarizing optics,
2. reflective collimator optics to avoid change-of-index when going to vacuum,
3. monolithic zerodur optical bench,
4. zerodur and invar optical mounts.

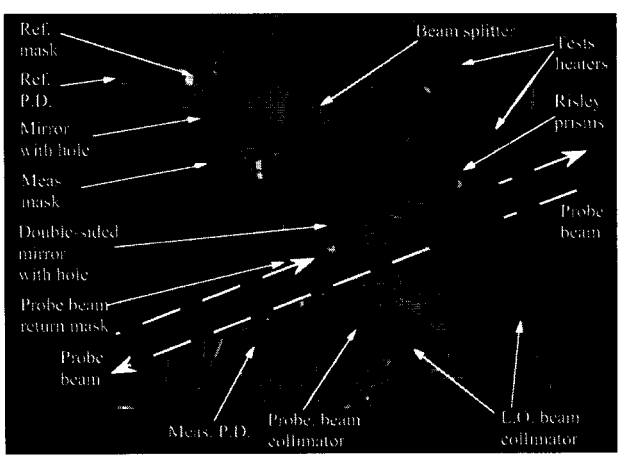

Fig. 4. Metrology head used in SIM testbeds. Heaters were placed on the rear and side surfaces of the zerodur bench supporting the optics.

Given this low-thermal expansion coefficient construction, we might expect a temperature sensitivity <0.1 pm/mK for uniform temperature change. Tests with the prototype in Fig 4 indicate an actual sensitivity of 7.7 pm/mK which we believe is dominated by temperature gradients. We have noticed additional drift associated with the pump-down of the test chambers which we suspect is caused by teflon rings in the area of the beam splitters and Risley prism.

A third generation metrology head is currently being developed that will address this and other known flaws.

4.2 Drift Issues with Fiber Optics

Distribution of laser light to the SIM metrology gauges is via single mode polarization maintaining (PM) optical fibers. A well-known issue with these is the asymmetric optical path length dependence on polarization. Ideally, laser light entering the fiber should only be polarized in the "slow" axis of the fiber. In practice there is always a small component polarized in the orthogonal "fast" axis. This results in elliptically polarized light at the output of the fiber. Because of the thermal sensitivity of fibers, the output polarization angle can rapidly drift. Drifting polarizations cause unstable interference fringes, unstable metrology.

The solutions to this problem are

1. use of a non polarization dependent metrology head,
2. "cleaning up" the laser light polarization at the metrology head and
3. protecting the fibers from temperature changes,

Points 1 and 2 might seem contradictory, but although the metrology head now in use does not explicitly require a particular polarization, the Probe beam and L.O. beam polarizations must be consistent with each other for good fringe visibility. In addition, reflecting surfaces such as the retroreflectors will introduce small polarization dependent phase changes. Hence, care was taken (such as fusion splicing fiber-to-fiber connections rather than using standard connectors) to prevent light from leaking into the fiber's fast axis. Finally, the last three meters of fiber are *polarizing* fiber (PZ fiber) instead of PM fiber, to ensure that only the correct polarizations emerge from the collimators.

4.3 Low-Drift Phase Measuring Electronics

Significant progress has been made in making the electronics that handle the interferometer photodiode signals drift-free and insensitive to change in signal strength. This work is presented elsewhere at this conference[12].

4.4 Active Optical Alignment

For correct measurement of the distance L between corner cube retroreflector fiducials, the probe beam from a metrology head should be aimed parallel to the vector connecting the fiducials' vertices. Mispointing of the metrology head by an angle θ causes an error in the measured length

$$\varepsilon(L)=L\theta^2/2. \qquad (2)$$

For example, if L = 10 meters, and θ=1 μRadian, then the error will be -5 pm. Since the effect is quadratic, a small additional mispointing will quickly exceeded the error budget, hence active alignment is essential. First demonstrated for single gauges [13], active alignment is used in the Two-Gauge testbed and has further evolved in KITE, the ongoing demonstration of a SIM-like metrology truss.

Fig. 5 shows the alignment control loop, as implemented in KITE. The dashed box contains physical parts: piezoelectric (PZT) alignment actuators, metrology readout of L, and the target which is the instantaneous vector connecting the retroreflectors. The target moves due to external influences such as mechanical drift, but more importantly because of simulated slewing of the siderostat mirrors (to acquire various stars).

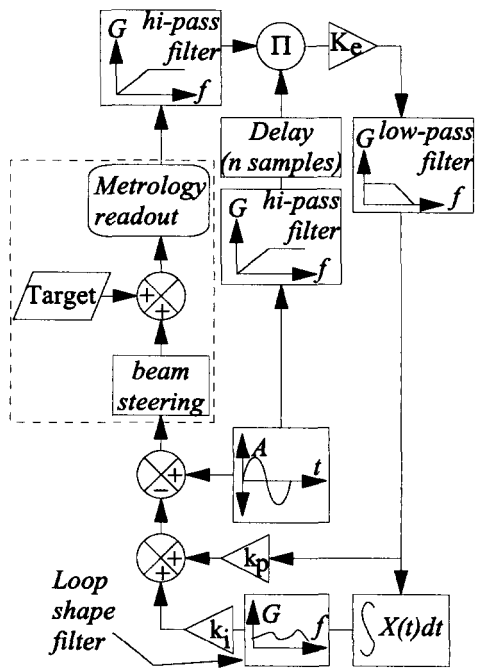

Fig. 5. Control loop for metrology head alignment. Two such loops, azimuth and elevation, are required per metrology head.

The pointing system in SIM's external metrology testbed, KITE, consists of a 2 degree of freedom (tip & tilt) PZT based fast steering actuator, a lock-in amplifier based pointing error sensor (tip and tilt) with delay compensation, and a control law designed to track linear drift. Fig. 5 shows the control loop for one degree of freedom only. The control law is a proportional integral (PI) controller with some loop shaping for improved tracking. The integrator in the loop is necessary for picometer performance given the type of drift observed in the testbed. Both the lock-in amplifier sensor and the control law are realized digitally at 1 kHz sample rates. In addition, the lock-in amplifier dithering frequency is picked such that measurement noise and structural dynamics are for the most part avoided. Currently, the dithering frequency

of choice is 6 Hz and the amplitude of dither is 50 micro-radians.

There are six gauges in KITE, and each is dithered at a different frequency (0.05 Hz separation in frequency is sufficient) to avoid cross talk. The lock-in amplifier sensor is a non-linear process, which is very sensitive to noise at the frequency of dither, transport delay and latencies in the system – these being the biggest drawbacks. However, when these drawbacks are dealt with adequately (i.e., reduce noise at dithering frequency, compensate for delay and latency) the sensor can be treated as a simple error sensor, which yields the error in pointing. The lock-in amplifier technique for KITE has been described in previous publications [13] and is not discussed here.

The pointing drift measured against a position sensitive detector is currently less than 5 micro-radians RMS/hour, with a closed loop bandwidth better than 1 Hz. Applying equation 2, this suggests the pointing drift contribution in KITE is less than 4 pm. The relatively high bandwidth allows the system to remain engaged at all times, even when large pointing errors are introduced due to routine system operation.

4.5 Absolute Metrology

At the time of the previous ICSO conference, absolute metrology for SIM was under development. This is the process of resolving the half-integer wavelength ambiguity of the metrology gauges. The KITE implementation is described in [14] and results are summarized in table 2.

The desired 3 micron accuracy has proven difficult to achieve, partly because of the previously discussed instability in the current generation of metrology heads. The new metrology heads, together with improving electronics should resolve this issue.

Table 2. Summary of current absolute metrology performance for the KITE testbed.

Two color frequency difference	15 GHz
Synthetic wavelength	2 cm
Chop rate	1 ms per color (500 Hz)
Accuracy	10 microns (see text)

5. TESTING SIM METROLOGY WITH KITE

The KITE experiment is to validate the metrology truss concept that is to monitor the three-dimension shape of SIM. The simplify the problem, KITE is a two-dimensional experiment, but the lessons learned could be later transferred to the three-dimensional truss. The vertices of the retroreflectors must be co-planar (approximately horizontal) to 100 microns to allow the vertical dimension to be ignored. Currently the vertices are co-planar to ~30 microns.

Fig. 6 diagrams the KITE testbed. The metrology heads, the "quick prototype" (QP) version, measure the distance between an articulated corner cube (ACC) and triple corner cubes (TCC) and a fixed "planarity" corner cube (PCC). The longest dimension is 2.9 meters, about 1/4th of the SIM baseline.

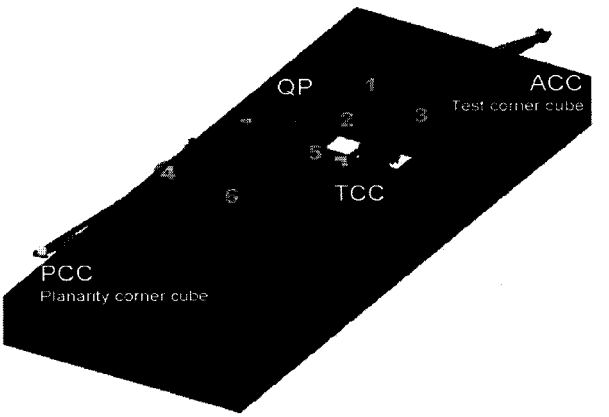

Fig 6. Diagram of the KITE testbed. The six metrology gauges interrogate 4 coplanar corner cube fiducials. The may be rotated and translated to simulate the motions of corner cubes mounted to SIM siderostats.

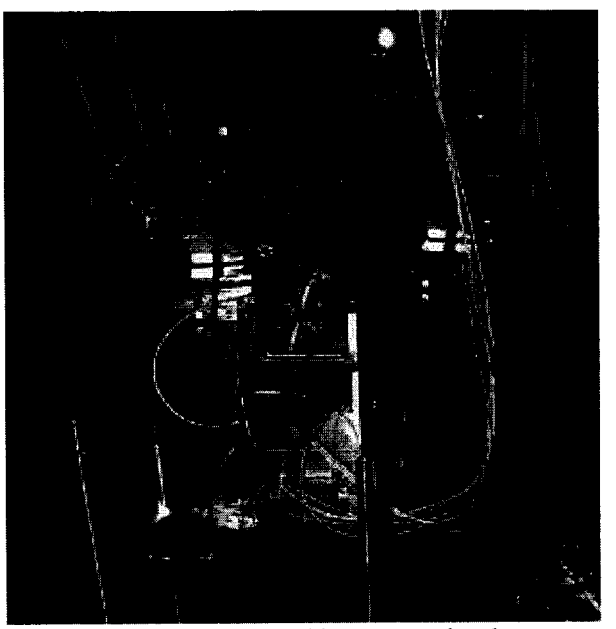

Fig.7. Photo of KITE testbed in vacuum chamber.

5.1 The KITE Metric

Fig. 8 diagrams KITE's six metrology measurements. Since six measurements L_1, L_2, .. L_6 over-defines the geometry, the longest measurement L_2 is treated as "truth" and can be compared with L_{2P}, the predicted length.

The KITE metric is the disagreement $\Delta \equiv L_2 - L_{2P}$ which should eventually be consistent with the SIM accuracy goals in Table 1.

Using the coordinate system defined in Fig. 8 the prediction L_{2P} can be calculated as follows:

$$X_2 = L_5, \qquad Y_2 = 0$$
$$X_1 = \frac{L_5^2 + L_3^2 - L_1^2}{2L_5}, \; Y_3 = \left(L_3 - X_1^2\right)^{1/2},$$
$$X_3 = \frac{L_5^2 + L_6^2 - L_4^2}{2L_5}, \; Y_3 = \left(L_6 - X_3^2\right)^{1/2}, \qquad (3)$$
$$L_{2P} = \left[(X_1 - X_3)^2 + (Y_1 - Y_3)^2\right]^{1/2}.$$

Note that the measurements L_N are the sum of the *absolute* (measured once at the start of a run) and *relative* distances (monitored in real-time).

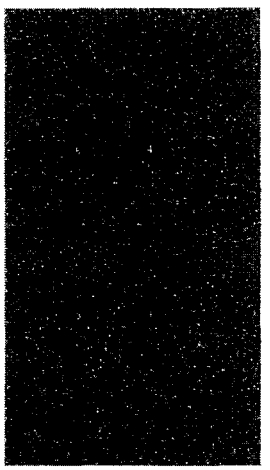

Fig. 8. Coordinate system for KITE metric.

5.2 KITE Results

KITE, as a representation of the SIM truss, was tested in two "astrometric observation" modes: narrow-angle (NA) and wide-angle (WA) as described in section 2. KITE's articulated corner cube (ACC) moved by amounts similar to the SIM siderostat-mounted cube in these modes. The data reduction included the removal of linear drifts, taking advantage of the chopped astrometric observation schedule. Also, the data reduction includes the removal of a systematic linear error due to the corner cubes dihedral error and the imprecise co-location of vertices in the triple corner cubes.

For the higher accuracy NA mode, the typically observed metric Δ is currently about 20 pm RMS, higher than the SIM goal of 10 pm. For the WA test Δ is currently about 215 pm, again higher than the SIM goal.

KITE's performance is expected to improve with the use of the next generation of metrology heads. These will have less drift, and are expected to accommodate higher pointing dither frequencies for more accurate active alignment.

KITE's electronics are also being upgraded to achieve lower drift and cyclic error.

6. CONCLUSION

SIM metrology has made significant strides. Table 3 summarizes the progress made thus far. It is anticipated that SIM's goal will be reached in the near future.

In interpreting the numbers in Table 3, it should be remembered that the NA and WA modes include rotations of the fiducials to simulate SIM observations, and also include the data processing which removes linear drifts and linear field-dependent errors (section 2).

Table 3. Metrology accuracies as measured by the KITE testbed. All values are RMS and include linear error removal (see text). KITE metrology goals are close to, but not identical to SIM goals due to scaling factors.

	Achieved in 2004	KITE Goal
Accuracy, NA mode	20 pm	8 pm
Accuracy, NA mode without motions	2.8 pm	5 pm
Accuracy, WA mode	215 pm	140 pm

7. ACKNOWLEDGEMENT

This research was carried out at the Jet Propulsion Laboratory, California Institute of Technology, under a contract with the National Aeronautics and Space Administration.

8. REFERENCES

1. *SIM, Taking the Measure of the Universe,* JPL publication 400-811 3/99. (Available online at sim.jpl.nasa.gov/library/book.html)

2. Laskin R.A., SIM Technology Development Overview: Light at the End of the Tunnel, *Interferometry in Space,Proceedings of the SPIE,* V. 4852, 16-32, 2003.

3. Halverson P.G., Progress Towards Picometer Accuracy Laser Metrology for the Space Interferometry Mission, *Proceedings of ICSO 2000, 4th International Conference on Space Optics,* 417-428, 12/2000, Toulouse, France.

4. Goullioud R., Wide Angle Astrometric Demonstration on the Micro-Arcsecond Metrology Testbed for the Space Interferometry Mission, *Proceedings of ICSO 2004, 5th International Conference on Space Optics* (this conference).

5. Dubovitsky S., Seidel D., Liu D., and Gutierrez R., Metrology source for high-resolution heterodyne interferometer laser gauges, *Proceedings of SPIE conference on Astronomical Interferometry*, V. 3350, 571–587, 1998.

6. Halverson P.G., Azevedo L.S., Diaz R.T., Spero R.E., Characterization of picometer repeatability displacement metrology gauges, *Proceedings of Optoelectronic Distance/Displacement Measurements and Applications (ODIMAP II)*, 63-68, Pavia, Italy, 9/2001

7. Unwin, S.C., SIM Science Operations, *Interferometry in Space, Proceedings of the SPIE*, V. 4852, 172-183, 2003.

8. Halverson P.G. and Spero R.E., Signal Processing and Testing of Displacement metrology Gauges with Picometre-scale Cyclic Nonlinearity, *Journal of Optics A: Pure and Applied Optics,* V.4, S304-S310, 2002.

9. Zhao F. et al., Development of Sub-nanometer Racetrack Laser Metrology for External Triangulation Measurement for the Space Interferometry Mission, *Proceedings of the Sixteenth Annual Meeting of the American Society for Precision Engineering*, Nov. 10-15 2001, Arlington Virginia, pp 349-352.

10. Ames L.L. et al., SIM external metrology beam launcher (QP) development, *Interferometry in Space, Proceedings of the SPIE*, V. 4852, 347-354, 2003.

11. Gursel Y., Laser metrology gauges for OSI, *Proceedings of SPIE conference on Spaceborne Interferometry*, V. 1947, 188–197, 1993.

12. Halverson P.G. et al., Signal Processing for Order 10 pm Accuracy Displacement Metrology in Real-World Scientific Applications, *Proceedings of ICSO 2004, 5th International Conference on Space Optics* (this conference).

13. Logan J.E. et al., Automatic Alignment of a Displacement-Measuring Heterodyne Interferometer, *Applied Optics*, V. 41, 21 Page 4314-4317, 2002

14. Mason J.E., Absolute metrology for the KITE testbed, , *Interferometry in Space, Proceedings of the SPIE*, V. 4852, 336-346, 2003.

Final V 2.8
CL 04-594 MP

PROGRESS TOWARDS PICOMETER ACCURACY LASER METROLOGY FOR THE SPACE INTERFEROMETRY MISSION – UPDATE FOR ICSO 2004

Peter G. Halverson[1], Oscar Alvarez-Salazar[2], Alireza Azizi[3], Frank Dekens[4], Bijan Nemati[5], Feng Zhao[6]

[1] Jet Propulsion Laboratory (JPL), California Institute of Technology,
4800 Oak Grove Drive, Pasadena, CA 91109 U.S.A, Peter.G.Halverson@jpl.nasa.gov
[2] JPL, Oscar.S.Alvarez-Salazar@jpl.nasa.gov
[3] JPL, Alireza.Azizi@jpl.nasa.gov
[4] JPL, Frank.G.Dekens@jpl.nasa.gov
[5] JPL, Bijan.Nemati@jpl.nasa.gov
[6] JPL, Feng.Zhao@jpl.nasa.gov

ABSTRACT

The Space Interferometry Mission, scheduled for launch in 2010, is an optical stellar interferometer with a 10 meter baseline capable of micro-arcsecond accuracy astrometry. A mission-enabling technology development program conducted at JPL, has yielded the heterodyne interferometric displacement metrology gauges required for monitoring the geometry of optical components of the stellar interferometer, and for maintaining stable starlight fringes. The gauges have <20 picometer linearity, <10 micron absolute accuracy, are stable to <200 pm over the typical SIM observation periods (~1 hour), have the ability to track the motion of mirrors over several meters. We discuss the technology that led to this level of performance: low-cross-talk, low thermal coefficient optics and electronics, active optical alignment, a dual wavelength laser source, and a continuously averaging, high data rate phase measurement technique. These technologies have wide applicability and are already being used outside of the SIM project, such as by the James Webb Space telescope (JWST) and Terrestrial Planet Finder (TPF) missions.

1. INTRODUCTION

The Space Interferometry Mission (SIM) [1,2] will measure the angular positions of ~20000 astronomical objects (mainly stars) for the detection and characterization of planets, gravitational lensing events, black holes and other exotic phenomena. SIM will detect these by their influence on the angular position of the object observed. For example, an earth-sized planet orbiting a nearby star at 1 AU could be detected by the angular "wobble" of the star, about 1 μas (=4.8 picoradians).

SIM measures the relative angles of stars on the celestial hemisphere by observing two "guide" stars which determine the orientation of SIM itself, while the third, "science" star is measured. Each star's angular position is measured by measuring the starlight phase delay between a pair of telescopes joined in an interferometer. Hence to function, SIM needs three starlight interferometers. (A fourth is available for redundancy.)

Metrology is needed to

1. provide knowledge of the angles between each interferometer (called external metrology) and
2. to provide internal calibration of the optical delay in the starlight interferometers (internal metrology).

Fig. 1 is a cut-away view showing the four stellar interferometers (two guide, and two science) and the external metrology beams that link them together in a three-dimensional virtual "truss" of positional information.

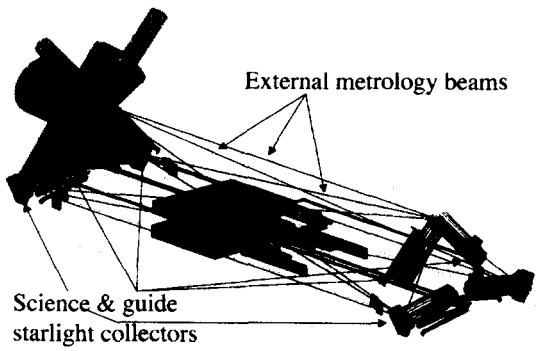

Fig. 1. SIM instrument layout. Blue indicates path of science starlight, green of guide starlight. Red indicates external metrology laser beams which measure distances between fiducials. The long dimension of the spacecraft is ~10 meters. Cones indicate the science and guide field-of-regard for the left side collectors. The right side field-of-regard cones, omitted for clarity, view the same portion of the sky.

The performance of SIM is directly related to the accuracy of the metrology. The error in measuring a star's location is roughly $\varepsilon(L)/D$ where $\varepsilon(L)$ is the typical metrology error and D=10 meters is the baseline, the distance between the starlight interferometer telescopes. For an astrometric accuracy of 5 picoradians, we would need to limit errors to 50

pm. Because of other error sources, the contribution from metrology should actually be less that this.

Table 1. SIM metrology requirements. Number in parentheses indicate *old* requirements, as of 2000.

	Internal metrology requirement	External metrology requirement
Number of gauges	4 (8)	19 (42)
Number of gauges for mission success*	3 (6)	12 (24)
Distance between fiducials	20 m	Shortest: 2.5 m (4 m) Longest: 10.6 m (12 m)
Motion; ranges of distances	~2.6 m	~10 microns
Velocity, internal	2 cm/s while changing stars, 1 micron/sec while observing	
Accuracy (absolute)	Not needed.	3 microns rms
Accuracy relative	~57 (15) pm rms, 1 hour time scale; ~10 (8) pm rms, 90 s time scale, *after removal of linear component***	
Temp. coefficient	2 pm/mK (soak); 50 pm/mK (sensitivity to gradients)	

* Assumes dispersed failures. Some failures are more tolerable than others.

** Modified observing schedule will allow off-line removal of drifts that are linear in time; further error removal based on instrument modeling should be possible.

Hence the metrology needs of SIM, listed in Table 1, are demanding and must be addressed for the mission to succeed. Early progress was described in the previous ICSO conference [3] and more of the real issues will be seen in another talk at this conference [4]. SIM metrology is still evolving in the laboratory and its final configuration is not yet known, but the lessons learned in ongoing experiments should apply.

It should also be noted that the accuracy requirements for a single gauge are relative to the other gauges, in the sense that if *all* gauges under/overestimate distances proportionally, the derived knowledge of the *angular shape* of SIM would be unaffected. Given that SIM's astrometric goals only require knowledge of the angles between the optical systems, to first order the need for laser source long-term wavelength stability is relaxed.

Although the distances the external metrology measures are several meters, the required dynamic range is small, a few microns, depending on the stiffness of the spacecraft.

Internal metrology has accuracy requirements similar to external metrology's but with a dynamic range of a few meters due to optical delay line motion. Because the internal metrology beam must coexist with the starlight, its aperture is constrained, causing diffraction induced errors which will be investigated by a separate experiment, the Diffraction Testbed [5].

1.1 General description of SIM metrology

Displacement metrology for the SIM testbeds (see Fig. 2) consists of a laser source [6] which supplies two λ=1.3 micron outputs with a small frequency difference F_{HET} which can be anywhere from 2 to 1000 kHz, the range of the phasemeter. The two frequency outputs serve as local oscillator (LO) and Probe sources. These outputs are carried to a metrology interferometer head (not to be confused with the *starlight* interferometers) by polarization maintaining (PM) fibers. If the experiment is inside a vacuum chamber, the fibers travel though a vacuum port to reach the metrology interferometers. The final three meters use *polarizing* fiber to remove energy from the "wrong" (fast) polarization axis before reaching the interferometers. The reason for this will be discussed later.

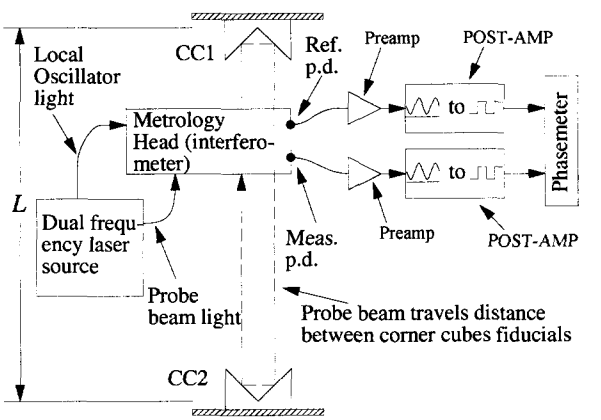

Fig. 2. Metrology gauge for measuring a single distance *L*. SIM uses 19 such gauges for external metrology and 4 for internal, starlight path, metrology.

Fig. 2 shows only one metrology gauge, but SIM will have 19 external gauges, which must work together to create a consistent three-dimensional shape, accurate to a few tens of picometers. The first step in showing that such a truss could be built was demonstrating close agreement between *pairs* of gauges. This was done in the Two-Gauge testbed [7], whose results are that the current gauges have

1. non-linearity < 22 pm for 10 micron displacements,

2. thermal sensitivity ~8 pm/mK,
3. drift ~300 pm/hour.

It should be noted that the cause of the drift is understood and will be corrected and that because of changes in the way the metrology data will be used, it would not be fatal to SIM even if it persisted. Similarly, we believe the thermal sensitivity can be easily reduced in the next generation of gauges.

1.2 Developments in SIM metrology

SIM metrology has evolved since the previous ICSO conference in the following significant ways:

1. Improvement in the astrometric observing plan now allow substantial (~85% to 90%) removal of metrology drift that is linear in time. Similarly, errors that are linearly dependant on observing direction can be mostly removed in data analysis [8].
2. To reduce cyclic non-linearity, the use of polarization as a means to control probe and reference beams has been replaced with physical beam separations.
3. Active alignment of metrology beams has been successfully implemented.
4. Numerous improvements in the electronics and data processing.
5. The metrology has been to scaled to various large testbeds, and has successfully been implemented as part of a SIM-like truss.

2. IMPROVED OBSERVATION SCHEDULE AND ANALYSIS

The order in which astrometric observations are performed has a strong impact on the required stability of the instrument. If the metrology drifts linearly with time, then by "chopping" the observations, alternately observing reference stars and science stars, the metrology error can be removed off-line.

An analogy would be having a meter stick that is growing, but also having a stable reference. We could accurately measure an unknown object with the meter stick by (1) measuring the reference then (2) measuring the unknown and (3) re-measuring the reference. If the time between measurements is constant (or at least known), then we can accurately calculate the unknown length.

In SIM's "narrow-angle" mode [8], which will have 5 picoradian accuracy, the positions of a science star, S, and a group of 5 nearby (within 1 degree) reference stars, R_1, R_2 .. R_5, will be measured in the sequence S-R_1-S-R_2-S-R_3-S-R_4-S-R_5-S. The time between each observation will be ~90 seconds. From the data thus acquired, linear drifts (and also linear field dependencies) will be removable. Hence, the modified SIM error budget allows for linear metrology drift. Of course, an "accelerating" drift would be problematic, and its effect must be less than 10 pm in 90 seconds.

SIM's "wide angle mode," accurate to 18 picoradians, is similar but with longer times scales to accommodate more targets. Within a 15 degree field of view, 6 grid (reference) stars G_1, G_2 .. G_6 will be measured, followed by N science stars S_1, S_2 .. S_N, followed by a repeated observation of the grid stars. The time scale for this sequence is ~1 hour, during which the non-linear, "accelerating," part of metrology drift must be less than 57 pm.

These observing sequences have been incorporated into the KITE testbed which will be discussed in section 5.

3. MINIMIZING CYCLIC ERROR

An early obstacle to <100 pm accuracy was cyclic error, a repeating non-linearity periodic in $\lambda/2$ fiducial displacement caused by (1) leakage (crosstalk) between the L.O. and Probe beams, (2) electrical crosstalk between the Meas. and Ref. heterodyne signals and (3) computational errors arising from data age when tracking a changing distance. The RMS magnitude of the error from the first two effects may be roughly predicted [9] by the formula

$$\varepsilon = 2^{-1/2}(\lambda/2)(1/2\pi)(v/V) \qquad (1)$$
$$\approx(\lambda/18)(v/V)$$

Applying this formula with λ=1.3 μm, we find that any leakage or crosstalk above -80 dB will cause ~10 pm cyclic error. From a practical standpoint for SIM, we strive to keep the mixing from any single source below -90 dB so that all sources taken together will be less than -80 dB.

The Two-Gauge testbed was used to confirm the cyclic performance of the gauges: after all the improvements described here, the gauges had cyclic errors that ranged from ~40 pm to <10 pm (the detection threshold). The later production metrology heads had better cyclic error performance.

3.1 Cyclic Error Due to Beam Leakage

The redesigned metrology [10,11] interferometer shown in Figures 3 and 4 represents a departure from the early SIM design (see for example [12]) in that the separation of the L.O. and Probe beams is no longer accomplished using polarizing beams splitters. Indeed, in the new design, L.O.-Probe. crosstalk is hardly an issue. However in this design, the probe beam is subdivided into an outer portion that travels between the fiducials and an inner portion that remains inside the head. These will form the Meas. and Ref. signals and any leakage (diffraction and scattering could be causes) between inner and outer beams is a potential new cause of cyclic error. Masks have been added to

reduce this leakage to acceptable levels. (The improved cyclic error of the later metrology heads was due to better diffraction blocking masks.)

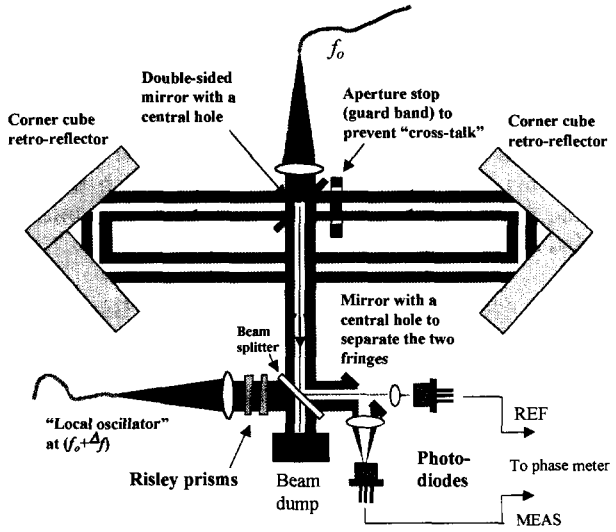

Fig. 3. Block diagram of metrology interferometer. Leakage between the outer beam, which measures distance between corner cube fiducials, and the inner beam, which acts as a reference, results in cyclic error. Similarly, crosstalk between photodiode signals causes cyclic error.

3.2 Cyclic Error Due to Multiple Gauges

As the testing of SIM metrology becomes more realistic on testbeds such as KITE (section 5) new issues inevitably arise. A new source of cyclic error has been observed that is caused by multiple gauges interrogating a common corner cube fiducial as in Fig. 6 and 7 where, for example, gauges 1, 2 and 3 all interrogate the articulated retroreflector cube. If a speck of dust scatters gauge 1's Probe beam into gauge 2, then gauge 2 will experience a cyclic error of magnitude predicted by equation 1. Better than 80 dB gauge-to-gauge isolation is required for <10 pm performance. The solution to this problem will probably involve better control of scattered light and having gauges use non-overlapping portions of the retroreflectors.

3.3 Cyclic error due to electronic crosstalk

Equation 1 also applies to signal mixing downstream of the Ref. and Meas. photodiodes. A continuing effort to upgrade the signal cabling and electronics, which will be presented elsewhere at this conference [13] is resolving this problem.

3.4 Cyclic error due to data age

This problem was noticed while testing the improved, low cyclic error, metrology gauges. It arises when fiducials are moving, and the effective time of measurement is correlated with the instantaneous phase. This effect can be removed in software as described in [9]. It should be noted that this error and the method for its removal are specific to the phase measuring device used at JPL. For current quasi-static experiments such as KITE, the data age issue is not important but it will have to be accounted for in future testbeds, and in SIM itself, where there will be optical delay line motions to compensate for spacecraft orientation drift.

4. MINIMIZING DRIFT

Table 1 includes metrology drift requirements which, to be met, have required the use of low thermal coefficient optics and structures, and special consideration of fiber optics issues, phase measuring electronics and optical alignment.

4.1 Optical configuration for low drift

The metrology head, Figs. 3 and 4, used in SIM testbeds has evolved to the form described in [10,11] which now features

1. no polarizing optics,
2. reflective collimator optics to avoid change-of-index effects when going to vacuum,
3. monolithic zerodur optical bench,
4. zerodur and invar optical mounts.

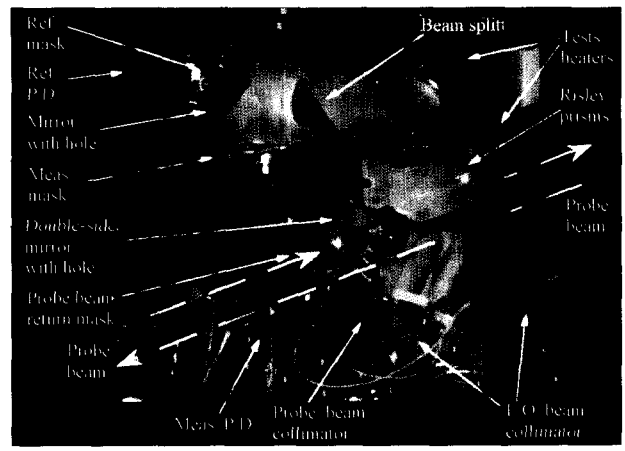

Fig. 4. Metrology head used in SIM testbeds. Heaters were placed on the rear and side surfaces of the zerodur bench supporting the optics to test thermal sensitivies.

Given this low-thermal expansion coefficient construction, we might expect a temperature sensitivity <0.1 pm/mK for uniform temperature change. Tests with the prototype in Fig 4 indicate an actual sensitivity of 7.7 pm/mK which we believe is dominated by temperature gradients. We have noticed additional drift associated with the pump-down of the test chambers which we suspect is caused by teflon rings in the area of the beam splitters and Risley prism. A third generation metrology head is currently being developed that will address this and other known flaws.

4.2 Drift Issues with Fiber Optics

Distribution of laser light to the SIM metrology gauges is via single mode polarization maintaining (PM) optical fibers. A well-known issue with these is the asymmetric optical path length dependence on polarization. Ideally, laser light entering the fiber should only be polarized in the "slow" axis of the fiber. In practice there is always a small component polarized in the orthogonal "fast" axis. This results in elliptically polarized light at the output of the fiber. Because of the thermal sensitivity of fibers, the output polarization angle can rapidly drift. Drifting polarizations cause unstable interference fringes, unstable metrology.

The solutions to this problem are

1. use of a non polarization dependent metrology head,
2. "cleaning up" the laser light polarization at the metrology head and
3. protecting the fibers from temperature changes,

Points 1 and 2 might seem contradictory, but although the metrology head now in use does not explicitly require a particular polarization, the Probe beam and L.O. beam polarizations must be consistent with each other for good fringe visibility. In addition, reflecting surfaces such as the retroreflectors will introduce small polarization dependent phase changes. Hence, care was taken (such as fusion splicing fiber-to-fiber connections rather than using standard connectors) to prevent light from leaking into the fiber's fast axis. Finally, the last three meters of fiber are *polarizing* fiber (PZ fiber) instead of PM fiber, to ensure that only the correct polarizations emerge from the collimators.

4.3 Low-Drift Phase Measuring Electronics

Significant progress has been made in making the electronics that handle the interferometer photodiode signals drift-free and insensitive to change in signal strength. This work is presented elsewhere at this conference[13].

4.4 Active Optical Alignment

For correct measurement of the distance L between corner cube retroreflector fiducials, the probe beam from a metrology head should be aimed parallel to the vector connecting the fiducials' vertices. Mispointing of the metrology head by an angle θ causes an error in the measured length

$$\varepsilon(L) = -L\theta^2/2. \qquad (2)$$

For example, if L = 10 meters, and θ=1 μRadian, then the error will be -5 pm. Since the effect is quadratic, a small additional mispointing will quickly exceed the error budget, hence active alignment is essential. First demonstrated for single gauges [14], active alignment is used in the Two-Gauge testbed and has further evolved in KITE, the ongoing demonstration of a SIM-like metrology truss.

Fig. 5 shows the alignment control loop, as implemented in KITE. The dashed box contains physical parts: piezoelectric (PZT) alignment actuators, metrology readout of L, and the target which is the instantaneous vector connecting the retroreflectors. The target moves due to external influences such as mechanical drift, but more importantly because of simulated slewing of the siderostat mirrors (to acquire various stars).

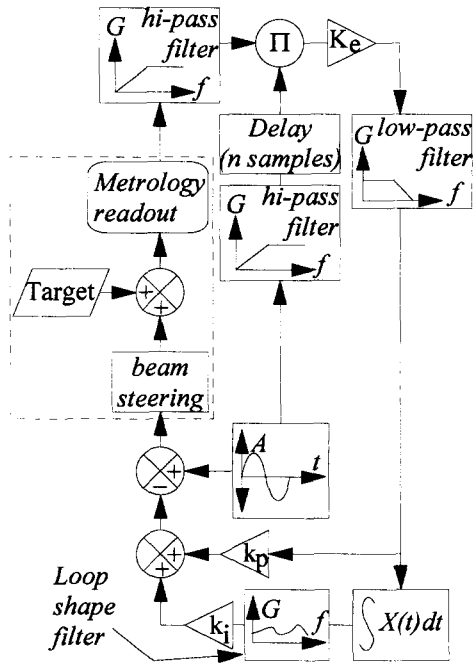

Fig. 5. Control loop for metrology head alignment. Two such loops, azimuth and elevation, are required per metrology head.

The pointing system in SIM's external metrology testbed, KITE, consists of a 2 degree of freedom (tip & tilt) PZT based fast steering actuator, a lock-in amplifier based pointing error sensor (tip and tilt) with delay compensation, and a control law designed to track linear drift. Fig. 5 shows the control loop for one degree of freedom only. The control law is a proportional integral (PI) controller with some loop shaping for improved tracking. The integrator in the loop is necessary for picometer performance given the type of drift observed in the testbed. Both the lock-in amplifier sensor and the control law are realized digitally at 1 kHz sample rates. In addition, the lock-in amplifier dithering frequency is chosen such that measurement noise and structural dynamics are for the most part avoided. Currently, the dithering frequency of choice is 6 Hz and the amplitude of dither is 50 micro-radians.

There are six gauges in KITE, and each is dithered at a different frequency (0.05 Hz separation in frequency is sufficient) to avoid cross talk. The lock-in amplifier sensor is a non-linear process, which is very sensitive to noise at the frequency of dither, transport delay and latencies in the system – these being the biggest drawbacks. However, when these drawbacks are dealt with adequately (i.e., reduce noise at dithering frequency, compensate for delay and latency) the sensor can be treated as a simple error sensor, which yields the error in pointing. The lock-in amplifier technique for KITE has been described in previous publications [14] and is not discussed here.

The pointing drift measured against a position sensitive detector is currently less than 5 micro-radians RMS/hour, with a closed loop bandwidth better than 1 Hz. Applying equation 2, this suggests the pointing drift contribution in KITE is less than 4 pm. The relatively high bandwidth allows the system to remain engaged at all times, even when large pointing errors are introduced due to routine system operation.

4.5 Absolute Metrology

At the time of the previous ICSO conference, absolute metrology for SIM was under development. This is the resolving of the half-integer wavelength ambiguity of the metrology gauges. The KITE implementation is described in [15] and results are summarized in table 2.

The desired 3 micron accuracy has proven difficult to achieve, partly because of the previously mentioned instability in the current generation of metrology heads. The new metrology heads, together with improving electronics should resolve this issue.

Table 2. Summary of current absolute metrology performance for the KITE testbed.

Two color frequency difference	15 GHz
Synthetic wavelength	2 cm
Chop rate	1 ms per color (500 Hz)
Accuracy	10 microns

5. TESTING SIM METROLOGY WITH KITE

The KITE experiment [16] is to validate the metrology truss concept that is to monitor the three-dimension shape of SIM. To simplify the problem, KITE is a two-dimensional experiment, but the lessons learned could be later transferred to the three-dimensional truss. The vertices of the retroreflectors must be co-planar (approximately horizontal) to 100 microns to allow the vertical dimension to be ignored. Currently the vertices are co-planar to ~30 microns.

Fig. 6 diagrams the KITE testbed. The metrology heads, the "quick prototype" (QP) version, measure the distance between an articulated corner cube (ACC) and triple corner cubes (TCC) and a fixed "planarity" corner cube (PCC). The longest dimension is 2.9 meters, about 1/4th of the SIM baseline.

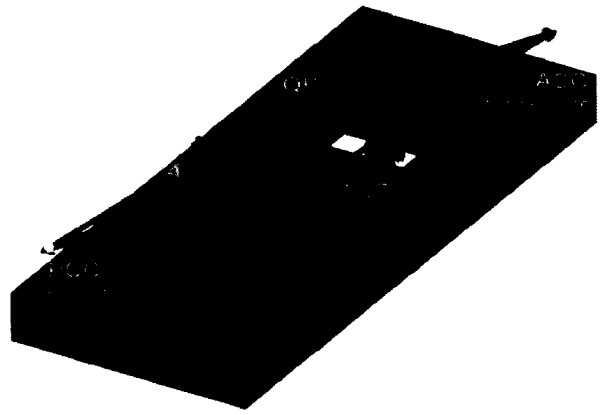

Fig 6. Diagram of the KITE testbed. The six metrology gauges interrogate 4 coplanar corner cube fiducials. The may be rotated and translated to simulate the motions of corner cubes mounted to SIM siderostats.

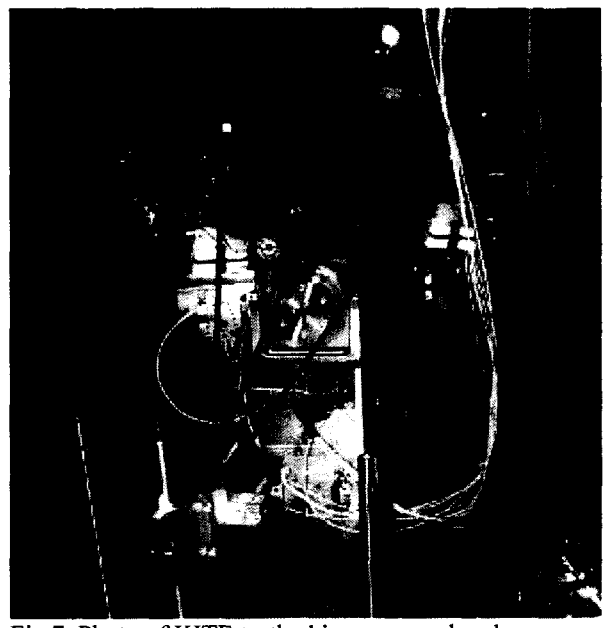

Fig.7. Photo of KITE testbed in vacuum chamber.

5.1 The KITE Metric

Fig. 8 diagrams KITE's six metrology measurements. Since six measurements L_1, L_2, .. L_6 over-defines the geometry, the longest measurement L_2 is treated as "truth" and can be compared with L_{2P}, the predicted length.

The KITE metric is the disagreement $\Delta \equiv L_2 - L_{2P}$ which should eventually be consistent with the SIM accuracy goals in Table 1.

Using the coordinate system defined in Fig. 8 the prediction L_{2P} can be calculated as follows:

$$X_2 = L_5, \qquad Y_2 = 0$$
$$X_1 = \frac{L_5^2 + L_3^2 - L_1^2}{2L_5}, \; Y_3 = \left(L_3 - X_1^2\right)^{1/2},$$
$$X_3 = \frac{L_5^2 + L_6^2 - L_4^2}{2L_5}, \; Y_3 = \left(L_6 - X_3^2\right)^{1/2}, \qquad (3)$$
$$L_{2P} = \left[(X_1 - X_3)^2 + (Y_1 - Y_3)^2\right]^{1/2}.$$

Note that the measurements L_N are the sum of the *absolute* (measured once at the start of a run) and *relative* distances (monitored in real-time). Note also that the accuracies quoted below will be based on Δ's divided by an appropriate scaling factor (typically ~1.4 to ~1.8) to apply to the context of SIM's metrology.

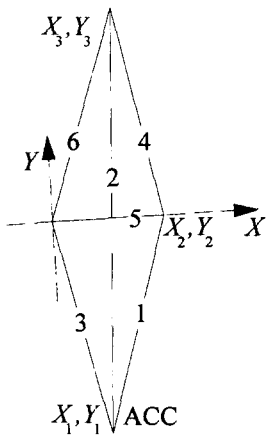

Fig. 8. Coordinate system for KITE metric.

5.2 KITE Results

KITE, as a representation of the SIM truss, was tested in two "astrometric observation" modes: narrow-angle (NA) and wide-angle (WA) as described in section 2. KITE's articulated corner cube (ACC) moved by amounts similar to the SIM siderostat-mounted cube in these modes. The data reduction included the removal of linear drifts, taking advantage of the chopped astrometric observation schedule. Also, the data reduction includes the removal of a systematic linear error due to the corner cubes dihedral error and the imprecise co-location of vertices in the triple corner cubes.

For the higher accuracy NA mode, the typically observed metric Δ is currently about 20 pm RMS, higher than the SIM goal of 10 pm. For the WA test Δ is currently about 215 pm, again higher than the SIM goal.

KITE's performance is expected to improve with the use of the next generation of metrology heads. These will have less drift, and are expected to accommodate higher pointing dither frequencies for more accurate active alignment.

KITE's electronics are also being upgraded to achieve lower drift and cyclic error.

6. CONCLUSION

SIM metrology has made significant strides. Table 3 summarizes the progress made thus far. It is anticipated that SIM's goal will be reached in the near future.

In interpreting the numbers in Table 3, it should be remembered that the NA and WA modes include rotations of the fiducials to simulate SIM observations, and also include the data processing which removes linear drifts and linear field-dependent errors (section 2).

Table 3. Metrology accuracies as measured by the KITE testbed. All values are RMS and include linear error removal (see text). KITE metrology goals are close to, but not identical to SIM goals due to scaling factors.

	Achieved in 2004	KITE Goal
Accuracy, NA mode	20 pm	8 pm
Accuracy, NA mode without motions	2.8 pm	5 pm
Accuracy, WA mode	215 pm	140 pm

7. ACKNOWLEDGEMENT

This research was carried out at the Jet Propulsion Laboratory, California Institute of Technology, under a contract with the National Aeronautics and Space Administration.

8. REFERENCES

1. *SIM, Taking the Measure of the Universe,* JPL publication 400-811 3/99. (Available online at sim.jpl.nasa.gov/library/book.html)

2. Laskin R.A., SIM Technology Development Overview: Light at the End of the Tunnel, *Interferometry in Space,Proceedings of the SPIE,* V. 4852, 16-32, 2003.

3. Halverson P.G., Progress Towards Picometer Accuracy Laser Metrology for the Space Interferometry Mission, *Proceedings of ICSO 2000, 4th International Conference on Space Optics,* 417-428, 12/2000, Toulouse, France.

4. Goullioud R., Wide Angle Astrometric Demonstration on the Micro-Arcsecond Metrology Testbed for the Space Interferometry Mission, *Proceedings of ICSO 2004, 5th International Conference on Space Optics* (this conference).

5. Schaechter, D.B. et al., Diffraction hardware testbed and model validation, *Interferometry in Space, Proceedings of the SPIE*, V. 4852, 302-313, 2003.

6. Dubovitsky S., Seidel D., Liu D., and Gutierrez R., Metrology source for high-resolution heterodyne interferometer laser gauges, *Proceedings of SPIE conference on Astronomical Interferometry*, V. 3350, 571–587, 1998.

7. Halverson P.G., Azevedo L.S., Diaz R.T., Spero R.E., Characterization of picometer repeatability displacement metrology gauges, *Proceedings of Optoelectronic Distance/Displacement Measurements and Applications (ODIMAP II)*, 63-68, Pavia, Italy, 9/2001

8. Unwin, S.C., SIM Science Operations, *Interferometry in Space, Proceedings of the SPIE*, V. 4852, 172-183, 2003.

9. Halverson P.G. and Spero R.E., Signal Processing and Testing of Displacement metrology Gauges with Picometre-scale Cyclic Nonlinearity, *Journal of Optics A: Pure and Applied Optics,* V.4, S304-S310, 2002.

10. Zhao F. et al., Development of Sub-nanometer Racetrack Laser Metrology for External Triangulation Measurement for the Space Interferometry Mission, *Proceedings of the Sixteenth Annual Meeting of the American Society for Precision Engineering*, Nov. 10-15 2001, Arlington Virginia, pp 349-352.

11. Ames L.L. et al., SIM external metrology beam launcher (QP) development, *Interferometry in Space, Proceedings of the SPIE*, V. 4852, 347-354, 2003.

12. Gursel Y., Laser metrology gauges for OSI, *Proceedings of SPIE conference on Spaceborne Interferometry*, V. 1947, 188–197, 1993.

13. Halverson P.G. et al., Signal Processing for Order 10 pm Accuracy Displacement Metrology in Real-World Scientific Applications, *Proceedings of ICSO 2004, 5th International Conference on Space Optics* (this conference).

14. Logan J.E. et al., Automatic Alignment of a Displacement-Measuring Heterodyne Interferometer, *Applied Optics*, V. 41, 21 Page 4314-4317, 2002

15. Mason J.E., Absolute metrology for the KITE testbed, , *Interferometry in Space, Proceedings of the SPIE*, V. 4852, 336-346, 2003.

16. Nemati B., External metrology truss technology demonstration (KITE), *Interferometry in Space, Proceedings of the SPIE*, V. 4852, 90-99, 2003.

Final V28
CL 04-595 MP

SIGNAL PROCESSING FOR ORDER 10 PM ACCURACY DISPLACEMENT METROLOGY IN REAL-WORLD SCIENTIFIC APPLICATIONS

Peter G. Halverson[1], Frank M Loya[2]

[1]Jet Propulsion Laboratory (JPL), California Institute of Technology, 4800 Oak Grove Drive, Pasadena, CA 91109 U.S.A., Peter.G.Halverson@jpl.nasa.gov
[2] JPL, Frank.M.Loya@jpl.nasa.gov

ABSTRACT

Projects such as the Space Interferometry Mission (SIM) [1] and Terrestrial Planet Finder (TPF) [2] rely heavily on sub-nanometer accuracy metrology systems to define their optical paths and geometries. The James Web Space Telescope (JWST) is using this metrology in a cryogenic dilatometer for characterizing material properties (thermal expansion, creep) of optical materials. For all these projects, a key issue has been the reliability and stability of the electronics that convert displacement metrology signals into real-time distance determinations. A particular concern is the behavior of the electronics in situations where laser heterodyne signals are weak or noisy and subject to abrupt Doppler shifts due to vibrations or the slewing of motorized optics. A second concern is the long-term (hours to days) stability of the distance measurements under conditions of drifting laser power and ambient temperature.

This paper describes heterodyne displacement metrology gauge signal processing methods that achieve satisfactory robustness against low signal strength and spurious signals, and good long-term stability. We have a proven displacement-measuring approach that is useful not only to space-optical projects at JPL, but also to the wider field of distance measurements.

1. INTRODUCTION

JPL's dimensional metrology challenges, typified by the efforts of the SIM metrology team [3],[4], TPF [5] and JWST [6] have forced the development of accurate phase measuring electronics to meet their metrology accuracy requirements which are listed in table 1.

This paper discusses signal processing downstream of the interferometer in Fig. 1, starting with the photo-diodes and continuing with preamps and integrated amplification, filtering and sine-to-square wave conversion devices called "post-amps" at JPL.

Since the laser wavelength λ is ~0.5 or ~1 micron and the accuracy $\varepsilon(L)$ needed is typically of order 10 picometers (pm), the heterodyne phases must be measured to $2\varepsilon(L)/\lambda \approx 2\text{x}10^{-5}$ cycles.

Table 1. Metrology needs of various project testbeds and experiments. TPF and SIM testbed metrology experiences will influence flight implementations. JWST's metrology need is for materials evaluation purposes only and will not be used in flight.

	JWST dilatometer	TPF	SIM
Laser λ	532 nm	1.5 μm	1.3 μm
Linearity	<50 pm	~100 pm	~10 pm
Stability	<50 pm	~100	~10 pm
Time scale	Days	~1000 s	hours

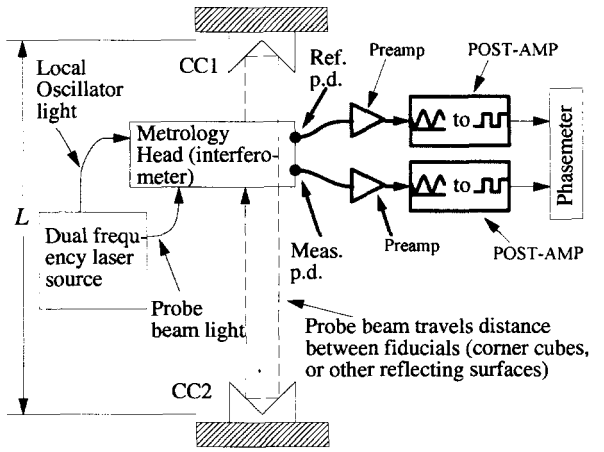

Fig 1. Context of the electronics discussed in this paper (bold). Heterodyne signals (2 kHz to 1 MHz) from the interferometer's photodiodes (p.d.) are amplified, filtered and converted to square waves by "post-amps". The phases of the square waves are measured by a phasemeter [7] and indicate L, the relative displacement of the fiducials in terms of the interferometer's laser wavelength.

2. LESSONS LEARNED

Our experience has shown that $\varepsilon(\phi) \approx 10^{-5}$ cycle accuracy phase measurements require care and attention to detail. Some of the obvious, and a few not-so-obvious lessons learned are summarized below:

1. *Shield the photodiode.* Many experiments have several cm long photodiode (p.d.) leads to keep heat-producing preamplifiers away from the optics. To avoid RF pickup, it is essential that the leads and diode be shielded with conductive braid or foil. See Fig. 2.

2. *Keep the photodiode capacitance low.* This is an old story but is worth repeating: any capacitance to ground at the inverting input of the op-amp will hugely increase the noise at the op-amp output. We have kept it low by

   a. making our own shielded cables to the p.d.'s by inserting loosely twisted "wire-wrap" wire (thin wire with low surface area) into a loose braid,
   b. selecting low capacitance p.d.'s,
   c. reverse biasing the p.d.,

in decreasing order of importance. See Fig. 2.

3. *Distribute the gain.* To keep the number of parts down, experimenters tend to want to amplify the (often tiny) photodiode signals to practical levels (~1 volt) in one or two op-amp stages. This is a bad idea if the gain per op-amp is higher than 1000 V/V or 10000 V/A or if the gain x F_{HET} approaches ~10% of the op-amp gain bandwidth product. To avoid parasitic oscillations and signal distortion, we are obliged to spread the gain across several op-amp circuits.

4. *Pay attention to op-amp slew rates.* An op-amp will begin to distort a sinusoid if the output voltage x frequency approaches ~10% of the device's slew rate. Such distortion causes high sensitivity to signal strength variations thus degrading phase stability.

5. *Buffer the signals.* After the initial gain stage after the photodiode (the transimpedance amplifier) there is typically several meters of cable to get out of the vacuum tank and to the instrument racks. That first amplifier's performance will be degraded (often unstable) if it drives that load. Much better performance is achieved with dedicated buffers, which can also incorporate voltage gain.

6. *Use differential signals.* For better spurious signal rejection, long cable runs can greatly benefit from differential drivers and receivers. Suitable monolithic *analog* differential drivers have not been available, so we made our own as in Figs 3 and 4.

7. *Avoid multiple grounds, ground loops.* This is needed for low cross-talk between channels. Any alternate route for a heterodyne signal to return to the instrument rack other than via its signal cable is an invitation to transmitting or receiving signals from adjacent channels, causing cyclic error. For example, if the photodiode shield happens to touch the optical table, a large (~100 pm) cyclic error can be expected.

8. *Isolate your electronics.* This is an extension of the previous point. Eliminate all common grounds between the photodiodes and phasemeters by running each photodiode, gain, filtering, and conversion to square waves processing chain on independent power supplies. Optically couple to the phasemeters, so each channel is floating. (In practice, it is necessary to bleed excess charge, so the grounds may connected to earth by 100 kOhm resistors.)

9. *Keep F_{HET}, the heterodyne frequency, low.* At high frequencies, cross talk increases, due to greater capacitive and inductive coupling. At high frequencies (above a few tens of kHz), the performance limits of op-amps are easily exceeded, resulting in distorted waveforms, and unexpected phase lags.

10. *Use wide bandpass filter frequencies.* A common mistake is to improve S.N.R. by installing a narrow bandpass around F_{HET}. This causes a large phase shift in the bandpass filter, which will vary with temperature. Keep the 3 dB points factors of >2 away from F_{HET}.

It should be noted that paying attention to the above points will also help eliminate "glitches", sudden integer cycle phase jumps caused by electrical noise (motors, lightning etc.).

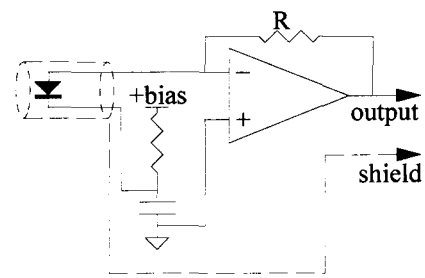

Fig. 2. Photodiode and transimpedance amplifier circuit with shielding. Note that the shield is distinct from circuit common.

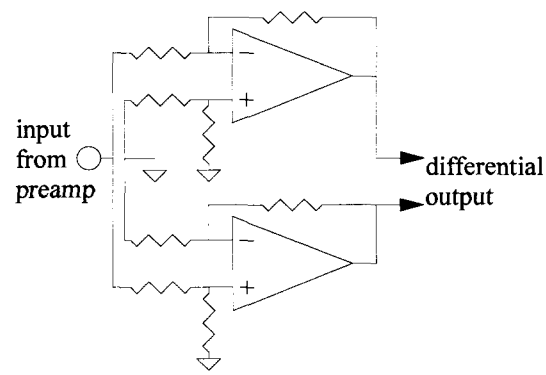

Fig. 3. Differential driver using two op-amps.

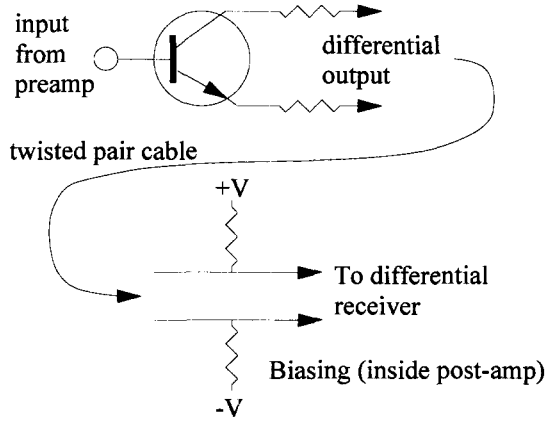

Fig 4. Differential driver using one transistor. This circuit [8] has very low heat dissipation, but requires bias at the receiving end of the cable.

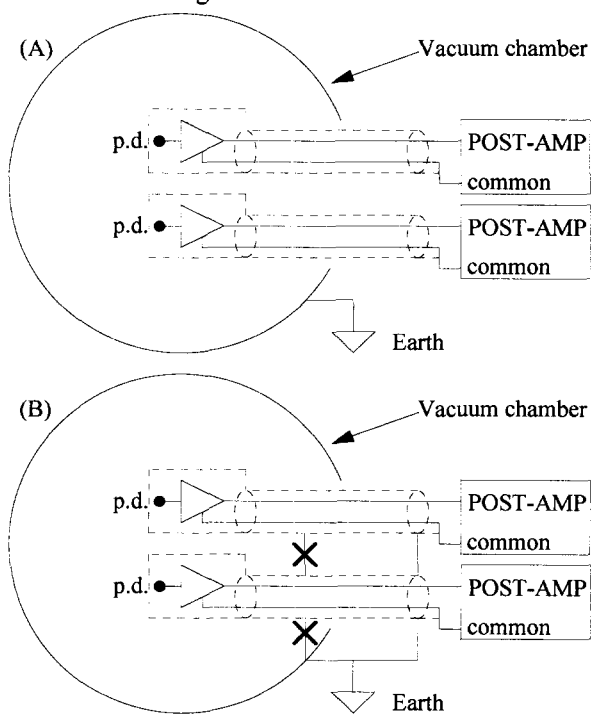

Fig 5. Shielding schemes, with shields shown in dashed lines. JPL experiments are typically in vacuum chambers, which are usually grounded. For low cross-talk and RF pickup, do "a". Don't do "b". In "a", the post-amp commons are shown disconnected, but if the output connections are not isolated, then the commons will link at the phasemeter. If the outputs *are* isolated (as in the new JWST/TPF post-amp), then it *might* be helpful to link the commons and possibly connect them to earth.

3. DRIFT ISSUES

Long-term stability of $\sim 10^{-5}$ cycles is challenging. The major obstacles are signal-strength variation coupling to phase error, and the thermal stability of the electronics.

(It might be noted that common-mode drift of all the channels, as would be caused by laser wavelength drift is not as much of a problem for current applications. We are concerned here with drift of a given channel relative to the others.)

3.1 Laser signal strength variation and zero-crossing level.

Fig. 6 shows the conversion from sinusoid to square wave. At JPL, the device that performs this function is called a "Post-Amp" and we will use this term. (Post-amps also perform signal amplification and conditioning, so the name is reasonable.)

The amplitude of the sine wave input is proportional to the laser power and to the interferometric fringe contrast which, in real-world systems, can be expected to vary a few percent. (This is particularly true for fiber-optic coupled interferometers, where temperature changes affect polarization, affecting the fringe contrast.)

Since typical JPL testbeds have heterodyne signal amplitude drift R_A=5%, if we want $\varepsilon(\phi) \approx 10^{-5}$ cycle stability, the amplitude-to-phase coupling $d\phi/dR_A$ must be less than 2×10^{-4}.

The phase of the output square wave will not be affected by the input amplitude drift if

1. the input sine wave phase is itself constant and
2. the sine wave is undistorted (or at least symmetric) and
3. the sine wave and the comparator's input offset voltages are both zero (or at least equal).

Requirements 1 and 2 will be approximately satisfied if low-distortion op-amps [9] are used upstream and are operated at low enough gain and amplitude to be far from their slew-rate and gain-bandwidth limitations. Example: if the op-amp GBWP=10 MHz and FHET=100 kHz, then the G must be < 100, preferably less. Similarly, if the slew-rate R=10V/μs, the gain must be $< R/(2\pi F_{HET})$=16. Evidently, the slew rate limitation is the more constraining.

Requirement 3 is problematic since all electronics experience some DC drift with temperature changes. Op-amp output drift can be eliminated by AC coupling, but comparator input offset, which is usually zeroed using an external potentiometer, cannot be eliminated.

Quantitatively, a comparator offset voltage will cause a phase sensitivity

$$d\phi/dR_A=(1/\pi)(V_{offset}/V_{pp}) \qquad (1)$$

in units of cycles, and where V_{pp} is the comparator input amplitude. Example: if V_{pp}=2 Volts, and we rquire $d\phi/dR_A<2x10^{-5}$, then V_{offset} must stay within +/- 0.13 mV. A typical comparator offset temperature coefficient is 0.01 mV/C, so for this example a 13 C range would be acceptable, ignoring all other effects.

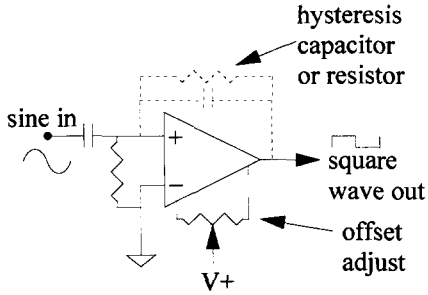

Fig. 6. Conversion of sinusoid to square wave. Dashed connections indicate optional hysteresis circuits.

The reader might suggest that using an automatic gain control (AGC) circuit would eliminate the amplitude variation problems just discussed, however it has proven difficult to construct an AGC circuit that doesn't introduce its own phase changes.

A practical obstacle in evaluating $d\phi/dR_A$ is that amplitude modulated sine wave sources that are free of phase modulation at the 10^{-6} level are not readily available. An approach we have found we can trust is shown in Fig. 7. Its advantage is that by using the same photodiode and electronics as in the final application, parasitic phase shifts are automatically taken into account.

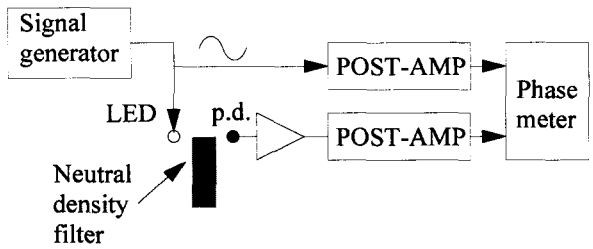

Fig. 7. Set up for testing amplitude-to-phase coupling. Signal generator set to F_{HET} drives LED and reference channel post-amp. Neutral density filter moved in/out of gap between LED and p.d., causes a varying amplitude but constant phase signal. The phase meter detects any spurious phase shift by comparing the two post-amp outputs.

3.2 Thermal stability of zero-crossing detector

Comparator offset drift $\varepsilon(V_{offset})$ will, by itself introduce a phase drift

$$d\phi/dV_{offset}=1/(\pi V_{pp}), \qquad (2)$$

in cycles. Example: V_{pp}=2 Volts, then for $\varepsilon(\phi)\approx10^{-5}$ cycles, $\varepsilon(V_{offset})$ must be less than .063 mV. If the comparator offset temperature coefficient is 0.01 mV/C, then a 6.3 C range would be acceptable, ignoring all other effects.

The offset drift problem will be worsened by the addition of a hysteresis feedback resistor (Fig. 6, needed for a glitch-free square-wave output) which will couple comparator output drift (or power supply drift) to the input. This can be solved by using a capacitor instead of a resistor. The capacitor value must be carefully chosen to provide enough feedback to debounce the output, but not so much as to noticably retard the output phase.

In practice, the current solution to the comparator drift problem is to stabilize the temperature, placing the electronics in a constant-temperature oven.

3.3 Thermal stability of bandpass filters

Another source of phase drift is the bandpass filters that are generally needed to remove RF pickup and noise from the photodiode signals. The circuit in Fig. 8 attenuates all frequencies outside of the band $\omega_{hp}<\omega_{HET}<\omega_{lp}$, where we are working in radians/s, $\omega\equiv2\pi F$. There is a phase shift associated with the high-pass and low-pass filters which change the phase by $\tan^{-1}(\omega_{hp}/\omega_{HET})$ and $\tan^{-1}(\omega_{HET}/\omega_{lp})$ respectively. ω_{hp} and ω_{lp} are determined by resistance and capacitance values which will drift with temperature. Low drift thin-film resistors are readily available, but even good quality capacitors [10] will drift ~0.01% per degree C.

The change in phase per change in capacitance can be predicted: Let $u=\omega_{hp}/\omega_{HET}$. A fractional increase in capacitance will cause an equal fraction decrease $\Delta u/u$, which will in turn cause a phase shift

$$\Delta\phi=u/(1+u^2)\ (\Delta u/u) \text{ radians.} \qquad (3)$$

Example: if F_{HET}=100 kHz, and the high-pass and low-pass frequencies are 50 kHz and 200 kHz respectively, so that for hi-pass u=1/2 and for low-pass u=2. A 0.01% change in capacitor values (as expected for a 1 degree change) will cause a phase shift
$\Delta\phi=(0.5)/(1+(0.5)^2)(0.0001)=4x10^{-5}$ radians
$=6.4x10^{-6}$ cycles.

An equal contribution *also* comes from the low-pass filter. Indeed, if there are N bandpass filters, the drift will be multiplied by $2N$. Increasing the bandpass width diminishes the phase shift. Using the previous example, doubling the frequency range to 25 to 400 kHz would reduce $\Delta\phi$ to $3.7\text{x}10^{-6}$ cycles.

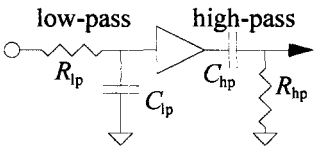

Fig. 8. Bandpass filter that allows through frequencies between $\omega_{lp}=R_{lp}C_{lp} > \omega > \omega_{hp}=R_{hp}C_{hp}$, radians/s. In practice, the buffer separating the low-pass and high-pass sections can be eliminated *if* $R_{lp} << R_{hp}$, (making it easy to modularise the bandpass filters).

4. GLITCHES

Because of the small photodiode currents (typically <1 μA, for ~2 μW impinging on the p.d.) the total gain from the front-end to the zero-crossing detector must be high (a few x 10^6 V/A in the bandpass frequencies). This large gain increases system susceptibility to technical noise: electric motors, radio stations etc. (Photodetector shot noise is also present, but is not an issue at these power levels.)

Technical noise tends to be impulsive, and it is very difficult to prevent it from causing unwanted zero-crossings which are seen as jumps (glitches) in phase of an integer number of cycles, which in turn cause problems for system control loops and complicate data analysis.

The cure for glitches is

1. paying attention to the previously discussed "lessons learned" and
2. increasing the AC current signal out of the photodiode (increasing the laser power, achieving better fringe contrast).

In our experience, narrowing the bandpass filters, and/or adding more filter stages does not help much. If cures 1 and 2 don't do the job, then phase-locked-loops can be used.

4.1 Glitch removal with phase-locked-loops

The addition of a phase-locked loop (PLL) [11] is a potent cure for glitches. Conceptually, the PLL is variable, voltage controlled frequency oscillator (VCO) with a mechanism that makes it closely follow the frequency and phase of the square wave from the zero crossing detector. In principle, the phase of the PLL output oscillator is equal to the zero-crossing phase plus a constant offset, usually 90 degrees. Input glitches are ignored by the PLL oscillator, which supplies a clean square wave to the phasemeter.

In practice, the phase relationship between the PLL input and output drifts with temperature. For the 74HC4046 we see roughly $2.5\text{x}10^{-4}$ cycles/C sensitivity. Further work should greatly improve this aspect of the circuit.

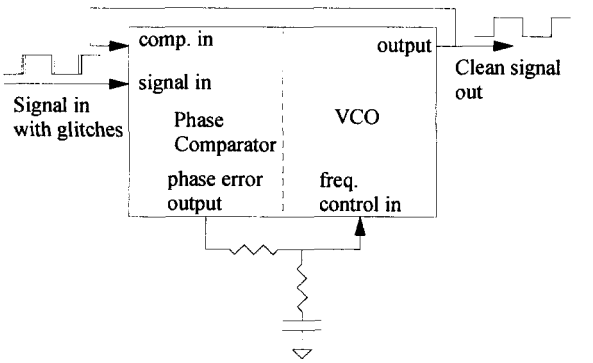

Fig. 9. Insertion of a PLL between the zero crossing detector and the phasemeter input, to remove glitches.

An additional benefit of the PLL technique is that it allows glitch-free measurement of low S/N signals, allowing much lower laser power. We are taking advantage of this in the JWST dilatometer where low sample heating, low incident power, are required.

5. CYCLIC ERROR, CROSSTALK

As previously mentioned, cross-talk between channels will cause a cyclic non-linearity in the measured phase. The approximate rms magnitude of this error is predicted [12] is the expression

$$\varepsilon(\phi) = 2^{-1/2}(1/2\pi)(V_l/V_{pp}) \approx (1/9)(V_l/V_{pp}), \qquad (4)$$

in cycles, where V_l is the amplitude of the leakage signal at the zero-crossing detector input and V_{pp} is the amplitude of the "good" signal. A spectrum analyser may used to measure the ratio V_l/V_{pp} where it will be typicaly expressed in dB. $R_{dB} = -20\log_{10}(V_l/V_{pp})$.

Example: a spectrum analyser monitoring the zero-crossing detector input shows that a "good" signal strength of 13 dBm and a leakage signal from the adjacent channel of -47 dBm. The 60 dB difference indicates that V_l/V_{pp} is 10^{-3}, hence the rms cyclic error will be about $0.9\text{x}10^{-3}$ cycles.

This level of leakage is typical of systems where ground loops, cabling, shielding and power supply distribution were not taken into consideration.

Applying the "lessons learned" will help get the 80 dB inter-channel isolation needed for 10^{-5} cycle accuracy.

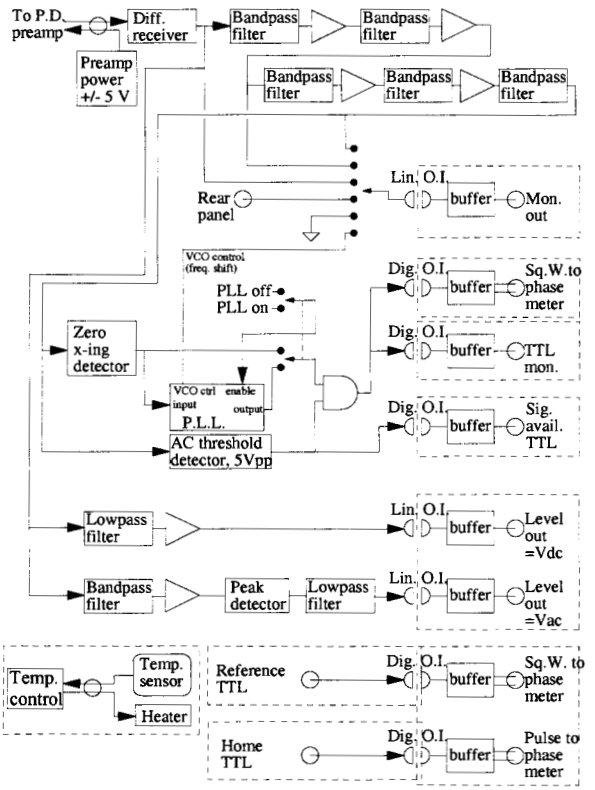

Fig. 10. Block diagram of JWST/TPF metrology post-amp. Dashed lines indicate boundaries of sections of the circuit that are isolated from each other, have separate floating grounds and independent power supplies to reduce cross-talk and to eliminate ground loops.

6. NEW POST-AMP DESIGN

A new signal-processing module (Figs 10, 11) incorporating all the "lessons learned" has been built and is in use by the JWST dilatometer and TPF nulling testbeds. Features of the post-amp include:

1. Incorporation of all the "lessons learned".
2. Electronics temperature regulated to 0.1 C for long-term stability.
3. Modular bandpass filters for easy changes in F_{HET}
4. Glitch removal using PLL circuits, user selectable.
5. All outputs optically isolated. No interconnected grounds.
6. Outputs including
   a. heterodyne signal waveform,
   b. fringe visibility (contrast) AC and DC components,
   c. PLL feedback,
   d. TTL and diffential square wave output.
7. Isolated power supply for photodiode preamp.
8. Bias for low heat dissipation single transistor differential driver (Fig. 4), user selectable.
9. Isolated interfaces for phase meter reference clock and HOME (integer phase reset) signal.

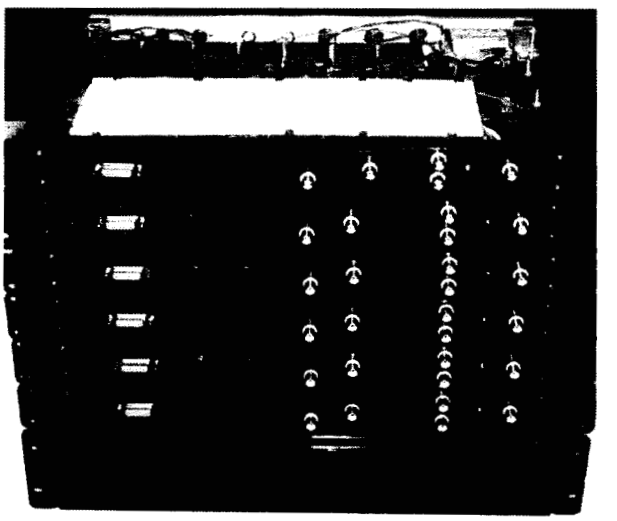

Fig 11. Photo of JWST/TPF metrology post-amps. Top module is open, showing multiple power supplies (rear) and the constant temperature oven (front). The bottom module is a six-channel temperature controller maintaining the ovens at 30.0 C.

7. POST-AMP RESULTS

The performance of the JWST/TPF post-amp are listed in table 2.

These performance data satisfy the needs of JWST, which uses a 532 nm laser. The expected long-term stability should be better than 10 pm, with the PLL in use and with temperature regulation.

More significantly, we have gained the ability to predictably achieve $\sim 10^{-5}$ cycle linearity and repeatability phase measurements of 2 kHz to 200 kHz heterodyne signals.

Table 2. Measured performance of JWST/TF post-amps.

		Notes
Frequency range	2 kHz to 200 kHz.	Diagnostic waveform output limit < 50kHz
Noise	2.2×10^{-8} $V/Hz^{1/2}$	Equivalent input noise.
Gain	1 to 2×10^{4}	
Filtering	5 bandpass	User defined
Phase locked-loop	Selectable on/off	Freq. and tracking user defined.
Thermal sensitivity	~2×10^{-5} cycles/C	No temp. control, no PLL.
Thermal sensitivity	~2.5×10^{-4} cycles/C	With PLL, no temp. control.
Temperature regulation	0.1 C	
Stability with temp control	~2×10^{-6} cycles	Expected, no PLL
Stability with temp control	~2.5×10^{-5} cycles/C	Expected, with PLL
Crosstalk	~-90dB	Typical, well-shielded signal cables.

8. ACKNOWLEDGEMENTS

The authors wish to acknowledge the hard work of Raymond Savedra who implemented many of the circuits discussed here and of Dorian Valenzuela and Guadalupe Sanchez who fabricated the new post-amps.

This research was carried out at the Jet Propulsion Laboratory, California Institute of Technology, under a contract with the National Aeronautics and Space Administration.

9. REFERENCES

1. *SIM, Taking the Measure of the Universe,* JPL publication 400-811 3/99 (Available online at sim.jpl.nasa.gov/library/book.html)

2. *The Terrestrial Planet Finder (TPF): A NASA Origins Program to Search for Habitable Planets,* JPL publication 99-003 4/99 (Available online at planetquest.jpl.nasa.gov/TPF/tpf_book/index.html

3. Goullioud R., Wide Angle Astrometric Demonstration on the Micro-Arcsecond Metrology Testbed for the Space Interferometry Mission, *Proceedings of ICSO 2004, 5th International Conference on Space Optics* (this conference).

4. Halverson P.G. et al., Progress Towards Picometer Accuracy Laser Metrology for the Space Interferometry Mission – Update for ICSO 2004, *Proceedings of ICSO 2004, 5th International Conference on Space Optics* (this conference).

5. Martin S., *A System Level Testbed for a Mid-infrared Beam Combiner for Terrestrial Planet Finder,* to be published in 2004 IEEE Aerospace Conf, March 2004, Big Sky, Montana, IEEEAC paper #1266

6. M. Dudik M. et al., Precision Cryogenic Dilatometer for James Webb Space Telescope Materials Testing, *Fifteenth Symposium on Thermophysical Properties,* June 2003, Boulder Colorado, http://symp15.nist.gov/pdf/p199.pdf

7. Halverson P.G. et al., *A Multichannel Averaging Phasemeter for Picometer Precision Laser Metrology,* Optical Engineering for Sensing and Nanotechnology (ICOSN '99) conference, 16-18 June 1999, Yokohama, Japan, Proceedings of the SPIE, V.3740, pp 646-649

8. Horowitz P. and Hill W., *The Art of Electronics, 2nd Ed.,* page 77, figure. 2.28, Cambridge University Press, Cambridge, U.K., 1989.

9. *OPA227, OPA228, High Precision, Low Noise Operational Amplifiers,* Burr-Brown (now Texas Instruments) product data sheet.

10. *ECHS PPS Film Capacitor,* Panasonic product data sheet.

11. *74HC4046A, High-Speed CMOS Logic Phase-Locked-Loop with VCO,* Fairchild (now Texas Instruments) product data sheet.

12. Halverson P.G. and Spero R.E., Signal Processing and Testing of Displacement metrology Gauges with Picometre-scale Cyclic Nonlinearity, *Journal of Optics A: Pure and Applied Optics,* V.4, S304-S310, 2002.